N,*N*′-Ethylenedi-L-cysteine (EC) and Its Metal Complexes: Synthesis, Characterization, Crystal Structures, and Equilibrium Constants

Yuejin Li,[†] Arthur E. Martell,*[,†] Robert D. Hancock,[§] Joseph H. Reibenspies,[†] Carolyn J. Anderson,[‡] and Michael J. Welch[‡]

Department of Chemistry, Texas A&M University, College Station, Texas 77843-3225, The Edward Mallinckrodt Institute of Radiology, Washington University School of Medicine, St. Louis, Missouri 63110, and Department of Chemistry, University of the Witwatersrand, Johannesburg, South Africa

Received November 17, 1994[⊗]

N,*N*′-ethylenedi-L-cysteine (EC) and its indium(III) and gallium(III) complexes have been synthesized and characterized. The crystal structures of the ligand and the complexes have been determined by single-crystal X-ray diffraction. EC·2HBr·2H_2O ($C_8H_{22}Br_2N_2O_6S_2$) crystallizes in the orthorhombic space group $P2_12_12$ with a = 12.776(3) Å, b = 13.735(2) Å, c = 5.1340 (10) Å, Z = 2, and V = 900.9(3) Å^3. The complexes Na[M(III)EC]·2H_2O ($C_8H_{16}MN_2O_6S_2Na$) are isostructural for M = In and Ga, crystallizing in the tetragonal space group $P4_22_12$ with the following lattice constants for In, (Ga): a = 10.068(2) Å, (9.802(2) Å), b = 10.068-(2) Å, (9.802(2) Å), c = 14.932(2) Å, (15.170(11) Å), Z = 4 (4), and V = 1513.6(5) Å^3, (1457.5(11) Å^3). In both metal complexes, the metal atoms (In and Ga) are coordinated by six donor atoms ($N_2S_2O_2$) in distorted octahedral coordination geometries in which two sulfur atoms and two nitrogen atoms occupy the equatorial positions, and the axial positions are occupied by two oxygen atoms of two carboxylate groups. The structures of the complexes previously predicted by molecular mechanics are compared with the crystal structures of the Ga(III) and In(III) complexes obtained experimentally. In contrast to the oxygen donors in phenolate-containing ligands, such as 1,2-ethylenebis((*o*-hydroxyphenyl)glycine) (EHPG) and *N*,*N*′-bis(*o*-hydroxybenzyl)ethylenediamine-*N*,*N*′-diacetic acid (HBED), the thiolate donors of EC enhances affinity for In(III) relative to Ga(III). The following stability sequence has been obtained: In(III) > Ga(III) ≫ Ni(II) > Zn(II) > Cd(II) > Pb(II) > Co(II). Evidence was also obtained for several protonated and hydroxo species of the complexes of both divalent and trivalent metals, where the corresponding protonation constants (K_{MHL}) decrease with increasing stability of the chelate, ML^{n-4}, where M^{n+} represent the metal ion.

Introduction

In a recent paper,[1] we reported a molecular mechanics simulation of the structures of the gallium(III) and indium(III) complexes of EC (*N*,*N*′-ethylene-di-L-cysteine), **1**. Now we are able to report the crystal structures of the Ga(III) and In(III) complexes of this ligand and to compare the results with the simulated structures. Although EC has been known for a long time,[2] and multidentate ligands containing thiolate donor groups have been of recent interest, we were surprised to learn that proton and metal ion affinities of EC have not been reported. The protonation constants and stability constants of the Ga(III) and In(III) chelates have recently been cited, but no experimental details were given.[1] In this paper the protonation of and metal ion complexation by EC in aqueous solution, including the complexation of a series of divalent metal ions, are described.

Many donor groups, such as phenolate, which impart high stabilities for the Fe(III) and Ga(III) chelates, do not do so in the case of In(III). The stability constants of complexes of *rac*-EHPG (1,2-ethylenebis((*o*-hydroxyphenyl)glycine), **2**, with log *K*'s of Fe(III), Ga(III), and In(III) of 35.54, 33.89, and 26.68,[3] and those of the corresponding metal complexes of HBED (*N*,*N*′-(*o*-hydroxybenzyl)ethylenediamine-*N*,*N*′-diacetic acid), **3**, are 39.01, 38.51, and 27.76,[4] respectively. The stability constants for indium(III) complexes are lower than those of iron-(III) and gallium(III) by as much as 7−11 orders of magnitude.[5] Indium(III) and Ga(III) are similar in their affinities for ligands with different donor groups. Estimated,[6] and experimental[7]

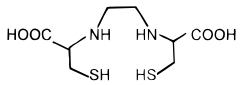

1 EC, H_4L

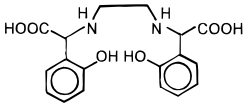

2 EHPG, H_4L

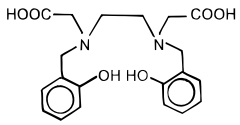

3 HBED, H_4L

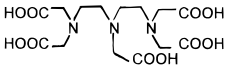

4 DTPA, H_5L

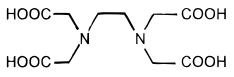

5 EDTA, H_4L

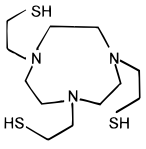

6 TACN-TM, H_3L

[†] Texas A&M University.
[‡] Washington University School of Medicine.
[§] University of the Witwatersrand.
[⊗] Abstract published in *Advance ACS Abstracts,* December 15, 1995.

(1) Anderson, C. J.; John, C. S.; Li, Y.; Hancock, R. D.; McCarthy, T. J.; Martell, A. E.; Welch, M. J. *Nucl. Med. Biol*. **1995**, *22*, 165.
(2) Crooks, H. M. In *The Chemistry of Penicillin*; Princeton University Press: Princeton, NJ, 1949; p 460.
(3) Bannochie, C. J.; Martell, A. E. *J. Am. Chem. Soc*. **1989**, *111*, 4735.
(4) Ma, R; Motekaitis, R. J.; Martell, A. E. *Inorg. Chim. Acta* **1994**, *224*, 151.
(5) Hancock, R. D.; Martell, A. E. *Chem. Rev*. **1989**, *89*, 1875.

0020-1669/96/1335-0404$12.00/0

values of log K_1 for Ga(III) and In(III) with unidentate ligands CH_3COO^-, RS^-, and saturated nitrogen donors, indicate the affinities of Ga(III) and In(III) for the donor atoms present on EC (Fe(III) is included for comparison):

metal ion	In(III)	Ga(III)	Fe(III)
log $K_1(CH_3COO^-)$[a]	3.4	3.8*	4.0
log $K_1(NH_3)$[a]	3.9*	3.7*	3.8*
log $K_1(RS^-)$[a]	9.6	8.7*	8.6*

[a] Experimental values: 25 °C, ionic strength zero; see ref 7. Estimated (*) values: see refs 5 and 6. R is $HOCH_2CH_{2-}$.

One should note that mercapto groups are not "soft" in the hard and soft acid base sense,[6] but should be regarded as possibly "borderline", and form complexes of high stability with such "hard" metal ions as Ga(III). In(III) and Ga(III) differ in size;[8] the ionic radius of Ga(III) is 0.55 Å, and that of In(III) is 0.80 Å (octahedral coordination). While the intrinsic strength of binding of these two ions to the individual donor atoms will be similar, the difference in size can lead to very different ligand selectivities, derived from steric effects.[9] The lower stability of complexes of the larger In(III) ion than of the smaller Ga(III) ion with *o*-hydroxybenzylate groups can be attributed to (1) the slightly lower affinity that In(III) has for negatively charged oxygen donor groups (indicated by log $K_1(OH^-)$ values of[7] In(III) = 10.0 and Ga(III) = 11.4), and (2) the size of the chelate rings. The six-membered chelate rings formed favor coordination of small metal ions such as Ga(III) and disfavor complexation of large metal ions such as In(III).[5,9]

Indium-111 ($T_{1/2}$ = 67.9 h) is a widely used radionuclide for nuclear medicine imaging. ^{111}In has a convenient half-life and it decays by electron capture with the emission of two photons at 173 keV (89%) and 247 keV (94%) which are ideal for gamma scintigraphy.[10] The 2.8 d half-life makes ^{111}In suitable for imaging with radiolabeled monoclonal antibodies (MAbs), which clear the circulation slowly. The most common bifunctional chelates used in complexing ^{111}In for labeling of MAbs include analogs of DTPA (diethylenetriaminepentaacetic acid), **4**.[11,12] Bifunctional chelates of HBED, **2**, have also been conjugated to MAbs and investigated *in vivo*.[13,14] One of the major problems with radiolabeled intact MAbs as radiopharmaceuticals is that a significant fraction of the radiometal is taken up and retained in the liver. Extensive work by our groups at Texas A&M and Washington University has shown that ^{111}In- or ^{67}Ga-labeled ligands show different liver clearance patterns depending on the stability of the metal-ligand complex.[1,15,16] In(III) or Ga(III) complexes that are of greater thermodynamic stability clear out of the liver and into the intestines, whereas less stable complexes remain trapped in the liver, possibly because of exchange with intracellular liver proteins. Maintaining high binding strength of ligands to Ga(III) and In(III) may be necessary to prevent exchange with natural receptors for trivalent metal ions such as the blood protein transferrin or other intercellular proteins in the liver.[17]

Experimental Section

Materials. All commercially available reagents used were of analytical grade. All solutions were prepared with distilled water that was deionized by means of an ion-exchange column from which oxygen and carbon dioxide were removed by boiling and subsequent cooling under argon. The metal salts were standardized complexometrically by either EDTA (ethylenediaminetetraacetic acid), **5**, titration with an appropriate indicator[18,19] or passage through Dowex 50W-X8 cation-exchange resin. In the latter case, the eluted acid was titrated with standard KOH solution. The base used for potentiometric titration was carbonate-free KOH solution, which was prepared from CO_2-free commercial concentrate (Baker "Dilut-it" ampules) and was standardized against oven-dried potassium hydrogen phthalate. A CO_2-free atmosphere for the base was maintained at all times.

Synthesis and Characterization of the Ligand. Ethylenebis-L-cysteine, **1**, was prepared via the reduction of L-thiazolidine-4-carboxylic acid by sodium in liquid ammonia.[2] Anal. Calcd (found) for $C_8H_{16}N_2O_4S_2$: C, 35.81 (35.42); H, 6.01 (5.96); N, 10.44 (10.15). Mass spectrum (FAB): *m/z* 267 $(M - H)^-$. ^{1}H NMR (in D_2O/DCl): 4.55 ppm (t, $-CH-$); 3.72 ppm (s, $-NCH_2CH_2N-$); 3.31 ppm (m, $-CH_2S-$).

Synthesis of Crystalline $H_4L\cdot 2HBr\cdot 2H_2O$, I. Single crystals of $H_4L\cdot 2HBr\cdot 2H_2O$ were grown as colorless needles from a hot aqueous 48% HBr solution upon slow cooling.

Synthesis of Crystalline Na[InEC]·2H$_2$O, II. To an aqueous solution of EC (54 mg, 0.20 mmol, 5 mL), was added 44 mg (0.20 mmol) of $InCl_3$. The solution was refluxed for 20 min after the pH value of the solution was adjusted to 7.5 with NaOH. The resulting solution was filtered. Cubic shaped, colorless single crystals of Na[InEC]·$2H_2O$ were grown from the filtrate on cooling to room temperature. Mass spectrum(FAB): *m/z* 379 $(M - H)^-$; 401 $(M + Na - H)^-$; 437 $(M + Na + 2H_2O - H)^-$. Electronic spectral band, λ_{max} (ϵ_{max}): 219 nm (1.61×10^4 dm^3 mol^{-1} cm^{-1}).

Synthesis of Crystalline Na[GaEC]·2H$_2$O, III. With the same procedure as that described for Na[InEC]·$2H_2O$, crystals of Na[GaEC]·$2H_2O$ were obtained. Mass spectrum(FAB): *m/z* 333 $(M - H)^-$; 355 $(M + Na - H)^-$; 391 $(M + Na + 2H_2O - H)^-$.

X-ray Crystallography. Single-crystal X-ray diffraction analyses were performed on EC·2HBr·$2H_2O$, Na[InEC]·$2H_2O$ and Na[GaEC]·$2H_2O$. The details of the data collection and structure refinement, the atomic coordinates, and the bond distances and angles for each compound are given in Tables 1−5, respectively.

A colorless needle (0.40 × 0.05 × 0.05 mm) for **I**, and colorless plates for **II** (0.25 × 0.25 × 0.25 mm) and **III** (0.05 × 0.15 × 0.20 mm) were each mounted on glass fibers with epoxy cement, at room temperature and cooled to 163 K for **I** and **II** and maintained at room temperature for **III**. Preliminary examinations and data collections were performed on a Rigaku AFC5R X-ray diffractometer (oriented graphite monochromator; Mo Kα (λ = 0.710 73 Å) radiation). Cell parameters were calculated from the least-squares fitting of the setting angles for 25 high-angle reflections ($2\theta_{av} > 20°$) The ω scans for several intense reflections indicated acceptable crystal quality.

Data were collected to 2 θ = 50° at 163 K for **I** an **II** and at room temperature for **III**. Scan width, on θ, for the data collection were $(1.628 + 0.3 \tan\theta)°$ for **I**, $(0.945 + 0.3 \tan\theta)°$ for **II**, and $(1.365 + 0.3 \tan\theta)°$ for **III**. Weak reflections were rescanned for a maximum of three scans to improve their individual counting statistics. Variable scan rates between 4 and 16°/min were employed. Three control reflections, collected every 150 reflections, showed no significant trends. Background measurements were made by the stationary crystal and

(6) Hancock, R. D.; Martell, A. E. *Adv. Inorg. Chem.*, in press.
(7) Smith, R. M.; Martell, A. E.; Motekaitis, R. J. *Critical Stability Constants Database*, Beta Version; NIST: Gaithersburg, MD, 1993.
(8) Shannon, R. D. *Acta Crystallogr.* **1976**, *A32*, 751.
(9) Hancock, R. D. *Progr. Inorg. Chem.* **1989**, *37*, 187.
(10) For a review, see: Anderson, C. J.; Schwarz, S. W.; Welch, M. J. in *Handbook on Metals in Clinical and Analytical Chemistry*; Seiler, H. G., Sigel, A., Sigel, H., Eds.; Marcel Dekker, Inc.: New York, 1994; pp 401−407.
(11) Hnatowich, C. J.; Layne, W. W.; Childs, R. L. *Int. J. Appl. Radiat. Isot.* **1982**, *33*, 327.
(12) Meares, C. F.; McCall, M. J.; Reardan, D. R.; Goodwin, D. A.; Diamanti, C. I.; McTigue, M. *Anal. Biochem.* **1984**, *142*, 68.
(13) Mathias, C. J.; Sun, Y.; Connett, J. M.; Philpott, G. W.; Welch, M. J.; Martell, A. E. *Inorg. Chem.* **1990**, *29*, 1475.
(14) Mathias, C. J.; Sun, Y.; Welch, M. J.; Connett, J. M.; Philpott, G. W.; Martell, A. E. *Bioconj. Chem.* **1990**, *2*, 204.
(15) Madsen, S. L.; Bannochie, C. J.; Martell, A. E.; Mathias, C. J.; Welch, M. J. *J. Nucl. Med.* **1990**, *31*, 1662.
(16) Madsen, S. L.; Bannochie, C. J.; Welch, M. J.; Mathias, C. J.; Martell, A. E. *Nucl. Med. Biol.* **1991**, *18*, 289.
(17) Madsen, S. L.; Welch, M. J.; Motekaitis, R. J.; Martell, A. E. *Nucl. Med. Biol.* **1992**, *19*, 431.
(18) Vogel, A. I. *A Textbook of Quantitative Inorganic Anaysis*, 3rd ed.; Longmans, Green and Co.: London, 1961.
(19) Schwarzenbach, G.; Flaschka, H. *Complexometric Titrations*; Metheun: London, 1969.

Table 1. Summary of Crystallographic data for **I**, **II**, and **III**

	I	**II**	**III**
empirical formula	$C_8H_{22}Br2N_2O_6S_2$	$C_8H_{16}InN_2NaO_6S_2$	$C_8H_{16}GaN_2NaO_6S_2$
fw	466.22	438.16	393.06
temp, K	163(2)	163(2)	293(2)
wavelength, Å	0.71073	0.71073	0.71073
cryst syst	orthorhombic	tetragonal	tetragonal
space group	$P2_12_12$	$P4_22_12$	$P4_22_12$
unit cell dimens[b]			
a, Å	12.776(3)	10.068(2)	9.802(2)
b, Å	13.735(2)	10.068(2)	9.802(2)
c, Å	5.1340(10)	14.932(2)	15.170(11)
vol, Å^3	900.9(3)	1513.6(5)	1457.5(1)
Z	2	4	4
density (calcd), g/cm^3	1.719	1.923	1.791
abs coeff (μ), mm^{-1}	4.752	1.889	2.227
final *R* indices [$I > 2\sigma(I)$][a]	R1 = 0.0363, wR2 = 0.0756	R1 = 0.0438, wR2 = 0.1196	R1 = 0.0674, wR2 = 0.1554
R indices (all data)[a]	R1 = 0.0618, wR2 = 0.1529	R1 = 0.0540, wR2 = 0.1274	R1 = 0.1966, wR2 = 0.3182

[a] $R1 = \sum||F_o| - |F_c||/\sum|F_o|$. $wR2 = \{\sum[w(F_o^2 - F_c^2)^2]/\sum[w(F_o^2)^2]\}^{1/2}$, where $w = [\sum^2(F_o^2) + (aF_o^2)^2 + (bF_o^2)]^{-1}$ where $a = 0.012$, 0.054, and 0.072 for **I**, **II**, and **III**, respectively, and $b = 0.936$, 9.26, and 7.54 for **I**, **II**, and **III**, respectively. $\alpha = \beta = \gamma = 90°$ for **I**, **II**, and **III**.

Table 2. Atomic Coordinates ($\times 10^4$) and Equivalent Isotropic Displacement Parameters (Å$^2 \times 10^3$)

	x	y	z	U(eq)
		I, $H_4L\cdot 2HBr\cdot 2H_2O$		
Br(1)	2160(1)	5047(1)	310(1)	28(1)
S(1)	7826(2)	7426(2)	−3921(6)	40(1)
O(1)	5207(5)	6532(4)	−3077(12)	43(2)
O(2)	5191(5)	7986(4)	−1200(10)	33(2)
O(3)	4494(4)	5876(4)	1332(5)	54(2)
N(1)	5918(4)	8926(4)	−5384(14)	30(2)
C(1)	6813(6)	7352(7)	−6334(19)	38(2)
C(2)	5798(6)	7838(6)	−5586(18)	31(2)
C(3)	4889(6)	9462(5)	−5559(15)	29(2)
C(4)	5367(6)	7480(6)	−3010(17)	28(2)
		II, $Na[InEC)\cdot 2H_2O$		
In(1)	5000	0	1400(1)	28(1)
Na(1)	0	0	1074(5)	142(6)
S(1)	4501(4)	2003(3)	529(2)	55(1)
O(1)	2801(7)	−90(8)	1712(4)	35(2)
O(2)	1174(7)	1318(8)	2051(5)	41(2)
O(3)	1303(15)	1303(15)	0	94(5)
O(4)	3194(29)	3194(29)	5000	296(30)
N(1)	4629(7)	1363(8)	2595(4)	18(2)
C(1)	3773(11)	2909(10)	1464(7)	33(2)
C(2)	3412(9)	2052(9)	2289(7)	26(2)
C(3)	4486(10)	555(10)	3420(5)	26(2)
C(4)	2382(10)	1019(11)	2010(7)	30(2)
		III, $Na[GaEc]\cdot 2H_2O$		
Ga(1)	0	5000	−1481(1)	23(1)
Na(1)	5000	5000	−1034(8)	175(11)
S(1)	307(4)	6841(4)	−552(3)	38(1)
O(1)	2117(9)	4858(11)	−1680(6)	26(2)
O(2)	3805(10)	6271(11)	−2029(8)	36(3)
O(3)	3200(16)	3200(16)	0	104(9)
O(4)	3685(14)	6315(14)	0	60(5)
N(1)	298(12)	6379(12)	−2536(8)	27(3)
C(1)	1116(15)	7892(15)	−1388(13)	42(5)
C(2)	1506(13)	7074(15)	−2208(12)	29(4)
C(3)	485(18)	5613(16)	−3361(10)	41(4)
C(4)	2588(17)	6028(16)	−1975(11)	30(4)

[a] U(eq) is defined as one-third of the trace of the orthogonalized U_{ij} tensor.

stationary counter technique at the beginning and end of each scan for 0.50 of the total scan time.

Lorentz and polarization corrections were applied to 877, 846, and 1525 reflections for **I, II**, and **III**, respectively. A semiempirical absorption correction was applied to **I** and **II**, and an empirical absorption correction was applied to **III**.[20] A total of 965, 835, and 1303 reflections for **I**, **II** and **III** were used in further calculations.

(20) PROCESS, Program for Data Reduction for Rigku AFC diffractometers. Molecular Structure Corp., The Woodlands, Texas.

Table 3. Bond Lengths (Å) and Angles (deg) for **I**[a]

S(1)−C(1)	1.794(9)	O(1)−C(4)	1.319(9)
O(2)−C(4)	1.182(9)	N(1)−C(2)	1.507(9)
N(1)−C(3)	1.509(9)	C(1)−C(2)	1.508(11)
C(2)−C(4)	1.515(12)	C(3)−C(3)[1]	1.505(13)
C(2)−N(1)−C(3)	113.1(6)	C(2)−C(1)−S(1)	114.8(6)
N(1)−C(2)−C(1)	111.7(7)	N(1)−C(2)−C(4)	107.4(7)
C(1)−C(2)−C(4)	113.1(7)	C(3)[1]−C(3)−N(1)	108.3(8)
O(2)−C(4)−O(1)	124.9(9)	O(2)−C(4)−C(2)	124.4(8)
O(1)−C(4)−C(2)	110.7(7)		

[a] Symmetry transformations used to generate equivalent atoms: (1) $-x + 1$, $-y + 2$, z.

Table 4. Bond Lengths (Å) and Angles (deg) for **II**[a]

In(1)−O(1)[1]	2.264(7)	In(1)−O(1)	2.264(7)
In(1)−N(1)	2.281(7)	In(1)−N(1)[1]	2.281(7)
In(1)−S(1)[1]	2.452(3)	In(1)−S(1)	2.452(3)
Na(1)−O(2)[2]	2.300(9)	Na(1)−O(2)	2.300(9)
Na(1)−O(3)[2]	2.45(2)	Na(1)−O(3)	2.45(2)
Na(1)−O(1)	2.979(7)	Na(1)−O(1)[2]	2.979(7)
Na(1)−Na(1)[3]	3.207(14)	S(1)−C(1)	1.823(11)
O(1)−C(4)	1.274(13)	O(2)−C(4)	1.254(13)
O(3)−Na(1)[3]	2.45(2)	N(1)−C(2)	1.480(11)
N(1)−C(3)	1.483(11)	C(1)−C(2)	1.547(14)
C(2)−C(4)	1.527(14)	C(3)−C(3)[1]	1.52(2)
O(1)[1]−In(1)−O(1)	156.3(3)	O(1)[1]−In(1)−N(1)	88.6(3)
O(1)−In(1)−N(1)	72.7(2)	O(1)[1]−In(1)−N(1)[1]	72.7(2)
O(1)−In(1)−N(1)[1]	88.6(3)	N(1)−In(1)−N(1)[1]	77.1(4)
O(1)[1]−In(1)−S(1)[1]	86.7(2)	O(1)−In(1)−S(1)[1]	106.1(2)
N(1)−In(1)−S(1)[1]	160.6(2)	N(1)[1]−In(1)−S(1)[1]	83.5(2)
O(1)[1]−In(1)−S(1)	106.1(2)	O(1)−In(1)−S(1)	86.7(2)
N(1)−In(1)−S(1)	83.5(2)	N(1)[1]−In(1)−S(1)	160.6(2)
S(1)[1]−In(1)−S(1)	115.87(14)	C(4)−O(1)−In(1)	111.2(7)
C(1)−S(1)−In(1)	95.0(3)	In(1)−O(1)−Na(1)	149.2(3)
C(4)−O(1)−Na(1)	76.8(6)	Na(1)[3]−O(3)−Na(1)	81.7(7)
C(4)−O(2)−Na(1)	109.2(7)	C(2)−N(1)−In(1)	100.1(5)
C(2)−N(1)−C(3)	115.7(7)	C(2)−C(1)−S(1)	115.2(7)
C(3)−N(1)−In(1)	109.6(5)	N(1)−C(2)−C(1)	108.2(7)
N(1)−C(2)−C(4)	109.1(8)	N(1)−C(3)−C(3)[1]	109.7(6)
C(4)−C(2)−C(1)	108.8(8)	O(2)−C(4)−C(2)	118.8(9)
O(2)−C(4)−O(1)	123.3(10)		
O(1)−C(4)−C(2)	117.8(9)		

[a] Symmetry transformations used to generate equivalent atoms: (1) $-x + 1$, $-y$, z; (2) $-x$, $-y$, z; (3) y, x, $-z$.

The structures were solved by direct methods.[21] Full-matrix least-squares anisotropic refinement on F^2 for all non-hydrogen atoms,[22] yielded R_1 of 0.036, 0.044, and 0.067 for **I**, **II**, and **III**, respectively, at convergence. Carbon-, nitrogen-, and sulfur-bound hydrogen atoms

(21) Sheldrick, G. *SHELXS-86 Program for Crystal Structure Solution*; Institut fur Anorganishe Chemie der Universitat: Gottingen, Germany, 1986.

Table 5. Bond Lengths (Å) and Angles (deg) for **III**

Ga(1)−O(1)	2.102(9)	Ga(1)−O(1)[1]	2.102(9)
Ga(1)−N(1)	2.115(11)	Ga(1)−N(1)[1]	2.115(11)
Ga(1)−S(1)[1]	2.308(4)	Ga(1)−S(1)	2.308(4)
Na(1)−O(2)	2.281(13)	Na(1)−O(2)[2]	2.281(13)
Na(1)−O(4)[2]	2.40(2)	Na(1)−O(4)	2.40(2)
Na(1)−O(3)	2.95(2)	Na(1)−O(3)[2]	2.95(2)
Na(1)−O(1)[2]	2.994(10)	Na(1)−O(1)	2.995(10)
Na(1)−Na(1)[3]	3.14(2)	S(1)−C(1)	1.82(2)
O(1)−C(4)	1.31(2)	O(2)−C(4)	1.22(2)
O(3)−Na(1)[3]	2.95(2)	O(4)−Na(1)[3]	2.40(2)
N(1)−C(2)	1.45(2)	N(1)−C(3)	1.47(2)
C(1)−C(2)	1.53(2)	C(2)−C(4)	1.52(2)
C(3)−C(3)[1]	1.53(3)		

O(1)−Ga(1)−O(1)[1]	163.4(5)	O(1)−Ga(1)−N(1)	78.3(4)
O(1)[1]−Ga(1)−N(1)	89.1(4)	O(1)−Ga(1)−N(1)[1]	89.1(4)
O(1)[1]−Ga(1)−N(1)[1]	78.3(4)	N(1)−Ga(1)−N(1)[1]	81.6(7)
O(1)−Ga(1)−S(1)[1]	99.5(3)	O(1)[1]−Ga(1)−S(1)[1]	90.6(3)
N(1)−Ga(1)−S(1)[1]	168.2(3)	N(1)[1]−Ga(1)−S(1)[1]	86.8(3)
O(1)−Ga(1)−S(1)	90.6(3)	O(1)[1]−Ga(1)−S(1)	99.5(3)
N(1)−Ga(1)−S(1)	86.8(3)	N(1)[1]−Ga(1)−S(1)	168.2(3)
S(1)[1]−Ga(1)−S(1)	104.8(2)	C(4)−O(1)−Ga(1)	109.8(9)
C(1)−S(1)−Ga(1)	94.3(5)	Ga(1)−O(1)−Na(1)	151.8(5)
C(4)−O(1)−Na(1)	74.9(8)	Na(1)[3]−O(3)−Na(1)	64.3(6)
C(4)−O(2)−Na(1)	110.6(11)	C(2)−N(1)−C(3)	115.3(12)
Na(1)[3]−O(4)−Na(1)	81.4(8)	C(3)−N(1)−Ga(1)	109.6(9)

C(2)−N(1)−Ga(1)	98.8(9)	N(1)−C(2)−C(4)	109.4(12)
C(2)−C(1)−S(1)	112.3(10)	C(4)−C(2)−C(1)	109.8(14)
N(1)−C(2)−C(1)	108.7(12)	O(2)−C(4)−O(1)	123.(2)
N(1)−C(3)−C(3)[1]	108.8(10)	O(1)−C(4)−C(2)	115.1(14)
O(2)−C(4)−C(2)	122.(2)	O(1)−C(4)−Na(1)	79.5(8)
O(2)−C(4)−Na(1)	46.6(9)		
C(2)−C(4)−Na(1)	155.1(12)		

were placed in idealized positions with isotropic thermal parameters fixed at 0.08 Å^2. No extinction correction was applied. Absolute configurations for all three structures were determined by examination of the Flack[23] absolute structure parameters (0.08(4), 0.1(2), and 0.02-(8) for **I**, **II**, and **III**, respectively. Neutral atom scattering factors and anomalous scattering correction terms were taken from ref 24.

General Techniques. ^{1}H NMR spectra in D_2O solution were measured on a Varian XL-200 spectrometer. The pD's of the D_2O solutions of the ligand were measured with a combination microelectrode. The $-\log [H^+]$ measurements were made after the calibration of the microelectrode with standard aqueous HCl solutions and the final pD was calculated by the equation pD = pH + 0.40.[25] Sodium 3-(trimethylsilyl)propane-1-sulfonate (DSS) was used as an internal standard. Negative-ion fast atom bombardment (FAB) mass spectra were determined with a VG Analytical 70S high resolution, double focusing, sectored (EB) mass spectrometer equipped with a VG Analytical 11/250J data system. Elemental analyses were carried out by Galbraith Laboratories, Inc., Knoxville, TN. UV absorption spectra were recorded with a Perkin-Elmer Model 553 fast scan spectrophotometer interfaced with a Perkin-Elmer R-1000 recorder.

Potentiometric Determinations. The potentiometric apparatus consisted of a Corning Research pH meter Model 130 fitted with glass (Sargent Welch) and calomel reference (Fisher) electrodes, a water-jacketed titration cell, a 10 mL capacity Metrohm piston buret which delivers standard KOH titration solution directly to the air-sealed cell through a buret tip which is secured to the cell cap with a clamp and O-rings, and a thermostated constant temperature bath set at 25.0 ± 0.1 °C. A stream of purified argon was used as the inert atmosphere in the titration cell and to degas all solutions before titrations. Oxygen and carbon dioxide were excluded from the reaction mixture by maintaining a slight positive pressure of purified argon in the titration cell. The last traces of oxygen were removed from the argon by passing it through an alkaline pyrogallol solution.

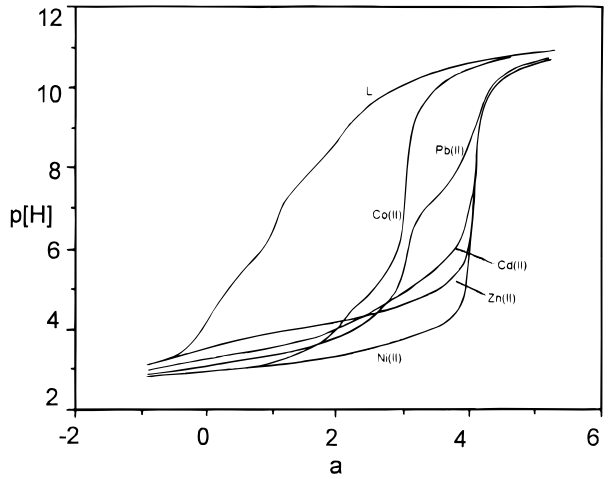

Figure 1. Potentiometric equilibrium curves of 1.00 × 10^{-3} M EC and EC complexes with divalent metal ions (as indicated). t = 25.0 °C, μ = 0.10 M (KCl), and a = moles of base added per mole of ligand.

The pH meter was calibrated to read p[H] directly prior to each potentiometric equilibrium experiment with a freshly prepared solution of standard dilute acid (HCl) at an ionic strength adjusted to 0.10 M with KCl. The day-to-day changes observed were on the order of <0.002 pH units at about p[H] 2.5. The term p[H] in this work is defined as $-\log [H^+]$, and the direct pH meter readings were used in the calculations of the equilibrium constants. The value of log $K_w([H^+][OH^-])$ used in the computations was found to be −13.78.[26]

The starting solutions for each potentiometric titration were prepared by adding successively to the titration cell, a required quantity of potassium chloride, a known volume of standard hydrochloric acid, metal chloride, and EC, and then the required amount of deionized distilled water. The ionic strength was adjusted to 0.10 M by the addition of KCl as supporting electrolyte, and solution concentrations of ligand and metal were in the order of 1 × 10^{-3} M. The protonation and stability constants were determined from two separate potentiometric titrations. A total of 60−90 points were collected for each experimental run.

The experimental p[H] values were plotted as a function of a values to obtain p[H] profiles for each system (Figure 1). An a value is the ratio of moles of base added per mole of ligand present, and a = 0 corresponds to the neutral form (H_4L) of the ligand. The protonation constants of EC and binding constants of EC with divalent metal ions Ni^{2+}, Zn^{2+}, Cd^{2+}, Pb^{2+}, and Co^{2+} were all determined by direct potentiometric titration. The equilibrium involving the formation of Ni(II) complexes was found to be relatively slow, and it was necessary to allow more than 30 min to reach equilibrium for each equilibrium point, in some pH ranges where the complexes were forming.

The complexation reactions of the trivalent metal ions, Ga^{3+} and In^{3+}, with the ligand, were found to be 100% complete over the accurately titratable range of p[H] 2−11. Thus ligand-ligand competition titrations were performed at the molar ratio mM:mL:mL′ = 1:1:1 for the determination of stability constants instead of direct potentiometric titration. EDTA, **5**, was used as the competing ligand L′ for both In(III) and Ga(III). Two-way approaches for determination of the stability constants were employed as follows. (1) $M^{III}EC-EDTA$: to a series of equilibrated 1:1 M(III)−EC solutions at the same $[H^+]$ were added a molar equivalent amount of EDTA and various amounts of acid, separately. (2) To a series of equilibriated 1:1 M^{III}−EDTA solutions at the same $[H^+]$ were added a molar equivalent amount of EC and various amounts of acid, separately. The above two approaches gave close results. Kinetic and potentiometric experiments indicate that the competition between EDTA and EC takes place in a limited pH range, but a long time is required to reach equilibrium for both

(22) Sheldrick, G. *SHELXL-93 Program for Crystal Structure Refinement*; Institut fur Anorganishe Chemie der Universitat: Gottingen, Germany, 1993.
(23) Flack, H. D. *Acta Crystallogr.* **1993**, *A39*, 876.
(24) *International Tables for Crystallography*; Wilson, A. J. C., Ed.; Kluwer Academic Publishers: Dordrecht, The Netherlands, 1992; Vol. C, Tables 6.1.1.4 (pp 500−502), 4.2.6.8 (pp 219−222), and 4.2.4.2 (pp 193−199).
(25) Glasoe, P. K.; Long, F. A. *J. Phys. Chem.* **1960**, *64*, 188.
(26) Martell, A. E.; Motekaitis, R. J. *Determination and Use of Stability Constants*, 2nd ed.; VCH Publishers: New York, 1992.

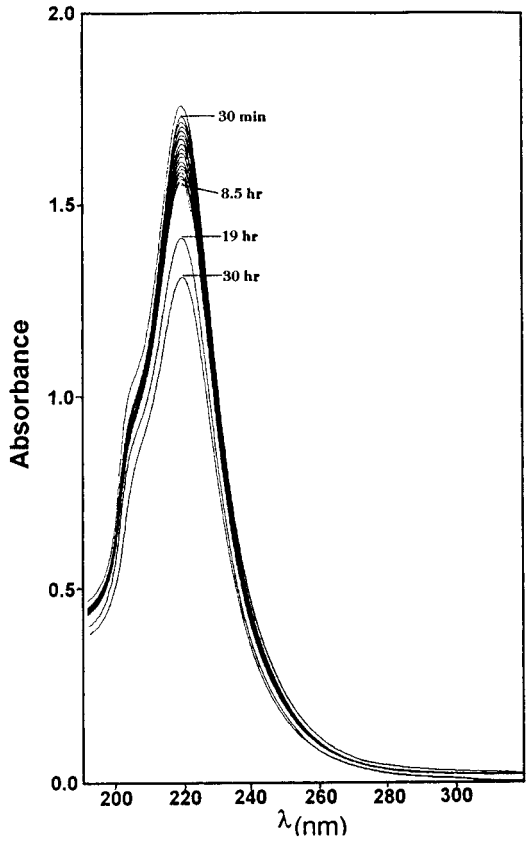

Figure 2. UV repeat-scan spectra showing the competition reaction of InEC (1.14×10^{-4} M and EDTA (1.33×10^{-4} M) at 25.0 °C, ionic strength 0.10 M (KCl) and pH 5.5. The recorded times shown in the Figure.

cases. Therefore, a batch procedure was performed. Figure 2 shows the spectral changes during the competition reactions of InEC (1.14×10^{-4} M) and EDTA (1.33×10^{-4} M) at 25 °C, ionic strength 0.10 M (KCl), and pH 5.5. More than 2 d were required to reach equilibrium.

Calculations. Ligand protonation constants and metal stability constants were calculated using the FORTRAN program BEST[26] and were obtained through the algebraic solution of mass balance and charge balance equations evaluated at each equilibrium point of the formation curves. The input for the program BEST consists of entering the components, the concentration of each component, and the initial estimate of the equilibrium constant for the formation of each species. The species considered present in the experimental solutions were those that one would expect to form according to established principles of coordination chemistry, and care was exercised to avoid the assumption of unnecessary species to improve the fit of the data. The program refines stability constants by iterative nonlinear least-squares fit of potentiometric equilibrium curves through a set of simultaneous mass balance equations for all the components expressed in terms of known and unknown equilibrium constants. By suitable use of the program, it is possible to obtain a high degree of discrimination in the selection of chemical species assumed for the unknown constants. Species distribution curves were calculated with the FORTRAN program SPE.[26]

Estimated Uncertainties. In the direct potentiometric titrations between p[H] 2 and 12, the σ_{fit}, which measures the difference between the experimental and calculated values of p[H], was found consistently to be 0.002−0.004 p[H] units. This has been increased to an estimated uncertainty of ±0.02 log units, to take into account uncertainties in weight of the sample, concentrations and volumes used of stock solutions, volume of titrant, etc. The estimated uncertainties are somewhat larger for solutions near and above p[H] 12 and near or below p[H] 2 because of variations of the liquid junction potentials. Also, for constants determined by competition with another ligand, and by the batch method, the agreement obtained between successive runs did not justify an estimated uncertainty of less than ±0.1 log unit.

Stability data taken from other sources and from the critical tables[7] are cited without estimated errors, but are considered reliable within ±1 unit of the last significant number shown.

Molecular Mechanics Calculations. These were carried out using the program SYBYL.[27] Sybyl models molecules by minimizing the total strain energy (ΣU) of the molecule, with contributions from bond length deformation strain energy (U_B), bond angle deformation strain energy (U_θ), torsional strain energy (U_ϕ), and van der Waals interactions between atoms not directly bonded to each other (U_{NB}).

$$\sum U = U_B + U_\theta + U_\phi + U_{NB}$$

Charges on atoms, calculated by *ab initio* or semiempirical methods, can be included, although this was not done here. Force field parameters for bonds between the metal ions In(III) and Ga(III) and the donor atoms N, O, and S were developed previously[1] for incorporation into the SYBYL force field. Unfortunately, the Cambridge Crystallographic Database (CCD) yielded only a few structures of complexes of In(III) and Ga(III) containing bonds of this type. Relevant structures are the TACN-TM (1,4,7-tris(2-mercaptoethyl)-1,4,7-triazacyclononane) complexes of Ga(III)[28] and In(III),[29] the EDTA complexes of Ga(III)[30] and In(III),[31] a TACN complex of In(III),[32] an In(III) complex of 1,4,7,10-tetraazacyclododecane-1,4,7-triacetate,[33] and the EHPG complex of Ga(III).[34] The search showed no structures with cysteine-type ligands with Ga(III) and In(III). The parameters in Table 6a gave good reproduction of the structures of In(III) and Ga(III) complexes.

There are two approaches to modeling geometry around metal ions.[9] In one, the L−M−L (L = ligand) bond angles are defined by appropriate ideal bond angles (90° for *cis* donor atoms and 180° for *trans* donor atoms in octahedral coordination) and force constants, while in the other approach no force constants apply to the L−M−L angles, and geometry around the metal ion is controlled by van der Waals repulsion between the donor atoms. The latter approach is advantageous with coordination numbers higher than six and the irregular coordination geometries often found in these situations. However, we found this approach not to work well for the large In(III) ion, since the donor atoms were too far apart to repel each other strongly and so control the geometry around the metal ion. For purposes of predicting geometry, it was found necessary to incorporate defined L−In−L bond angles and force constants. The previously developed[1] MM parameters for In(III) and Ga(III) were slightly improved by further small modifications. These parameters are reported in Table 6a. In Table 6b are shown calculated and observed structural parameters for the EC and TACN-TM complexes of Ga(III) and In(III).

Results and Discussion

X-ray Crystal Structures. Figure 3 shows a view and the atom-numbering scheme of the dication LH_6^{2+}, together with the two associated bromide ions and the two water molecules in the compound $H_4L \cdot 2HBr \cdot 2H_2O$. Crystal data and details of the crystal structure determination are given in Table 1. The crystal structure of EC has 2-fold symmetry, and the compound crystallizes in the orthorhombic space group $P2_12_12$ with a = 12.776(3) Å, b = 13.735(2) Å, and c = 5.134(10) Å. Figure 3 provides very important evidence for the characterization of the ligand by distinguishing it from an isomeric ligand (with the same elemental analysis) formed by S-alkylation of cysteine with ethylene dihalides.

(27) Clark, M.; Cramer, R. D.; van Opdenbosch, N. *J. Comput. Chem.* **1989**, *10*, 982.
(28) Moore, D. A.; Fanwick, P. E.; Welch, M. J. *Inorg. Chem.* **1990**, *29*, 672.
(29) Bossek, U.; Hanke, D.; Wieghardt, K.; Nuber, B. *Polyhedron* **1993**, *12*, 1.
(30) Kennard, C. H. L. *Inorg. Chim. Acta* **1967**, *1*, 347.
(31) Agre, V. M.; Kozlova, N. P.; Trunov, V. K.; Ershova, S. D. *Zh. Strukt. Khim.* **1979**, *22*, 138.
(32) Wieghardt, K.; Kleine-Boymann, M.; Nuber, B.; Weiss, J. *Inorg. Chem.* **1986**, *25*, 1654.
(33) Riesen, A.; Kaden, T. A.; Ritter, W.; Macke, H. R. *J. Chem. Soc., Chem. Commun.* **1989**, 460.
(34) Riley, P. E.; Pecoraro, V. L.; Corrano, C. J.; Raymond, K. N. *Inorg. Chem.* **1983**, *22*, 3096.

Table 6

(a) Parameters for Inclusion of Ga(III) and In(III) in the Molecular Mechanics Program SYBYL[a]

Bond Length Deformation Parameters

bond	strain-free length (Å)	force const (kcal mol^{-1} Å^{-1})	bond	strain-free length (Å)	force const (kcal mol^{-1} Å^{-1})
In−N	2.38	200	Ga−N	2.15	200
In−S	2.51	100	Ga−S	2.34	100
In−O	2.23	100	Ga−O	2.04	100

Bond Angle Deformation Parameters

bond angle[b]	ideal angle (deg)	force const (kcal mol^{-1} deg^{-2})	bond angle[b]	ideal angle (deg)	force const (kcal mol^{-1} deg^{-2})
N−In−N	90	0.005[c]	S−In−S	90	0.005[c]
N−In−S	90	0.005[c]	In−N−C	112	0.02
N−In−O	90	0.005[c]	In−S−C	97	0.02
O−In−O	90	0.005[c]	In−O−C	109.5	0.02
O−In−S	90	0.005[c]			

(b) Selected Bond Angles and Lengths Involving the Metal Ions from Complexes of In(III) and Ga(III) with the Ligands EC and TACN-TM, As Predicted by MM Calculation, and Observed[d]

	calcd	obsd		calcd	obsd		calcd	obsd
				cis-[In(EC)]$^-$				
				Bonds				
In−N	2.31	2.28	In−S	2.48	2.45	In−O	2.22	2.26
				Angles				
S−In−S	116.4	115.9	N−In−N	78.8	77.1	In−S−C	97.1	95.0
O−In−O	169.8	156.3	In−N−C	101.7	100.1	In−O−C	110.2	111.2
				cis-[Ga(EC)]$^-$				
				Bonds				
Ga−N	2.13	2.12	Ga−S	2.31	2.31	Ga−O	2.04	2.10
				Angles				
S−Ga−S	101.1	104.8	N−Ga−N	84.9	81.6	Ga−S−C	96.7	94.3
O−Ga−O	178.0	163.4	Ga−N−C	96.7	98.8	Ga−O−C	107.7	109.8
				[In(TACN-TM)]				
				Bonds				
In−N	2.32	2.40	In−S	2.50	2.52			
				Angles				
In−N−C	105.0	105.6	S−In−S	97.9	103.8			
N−In−N	78.9	74.5	In−S−C	98.9	99.3			
				[Ga(TACN-TM)]				
				Bonds				
Ga−N	2.15	2.20	Ga−S	2.33	2.34			
				Angles				
Ga−S−C	100.7	99.3	S−Ga−S	90.0	98.5			
N−Ga−N	86.9	78.9	Ga−N−C	101.4	105.4			

[a] SYBYL.[27] [b] The same force constants and angles were used for Ga(III). [c] These constants were set to zero when the approach for modeling the coordination geometry around the metal ion was adopted where van der Waals forces between the donor atoms determined the coordination geometry. [d] EC = *N,N′*-ethylenedi-L-cysteine, TACN-TM = 1,4,7-tris(2-mercaptoethyl)-1,4,7-triazacyclononane. Angles in degrees; lengths in Å. Calculated angles and lengths were obtained from the program SYBYL,[27] incorporating parameters in Table 6a.

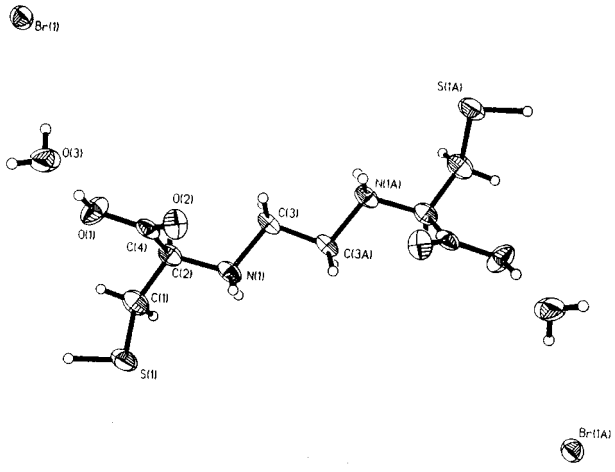

Figure 3. ORTEP diagram of H_6L^{2+} with the associated Br^- and H_2O, showing the atom-numbering scheme.

The indium and gallium complexes (Na[MEC]·2H_2O) were prepared from aqueous solution at neutral pH. The crystal structure of Na[InEC]2H_2O consists of $InEC^-$ anion, sodium ion, and two water molecules. The Na^+ ion interacts with several oxygen atoms(distance range 2.300(9) − 2.979(7) Å) of the carboxylate groups and the water molecules. The overall perspective view, as shown in Figure 4, illustrates the atom-labeling scheme of the $[In^{III}EC]^-$ anion. The coordination geometry around the indium atom is a distorted octahedron in which two sulfur atoms and two nitrogen atoms occupy the equatorial positions. The axial positions are occupied by two oxygen atoms of the two carboxylate groups. The two sulfurs are in cis positions to each other. Also prominent in the crystal structure of InEC complex is the symmetry in all the bond distances. The central In(III) atom lies on a 2-fold screw axis. The In−O, In−N, and In−S distances in each half of the Na-[InEC]·2H_2O molecule are equivalent, averaging 2.264(7), 2.281(7), and 2.452(3) Å, respectively. This is one of few In-(III)−sulfur complexes which have been isolated and structurally characterized. Bossek *et al*. have recently reported a crystal structure of the complex In(TACN-TM) with an N_3S_3 donor set.[29] The crystal structure of the EC complex of In(III) is

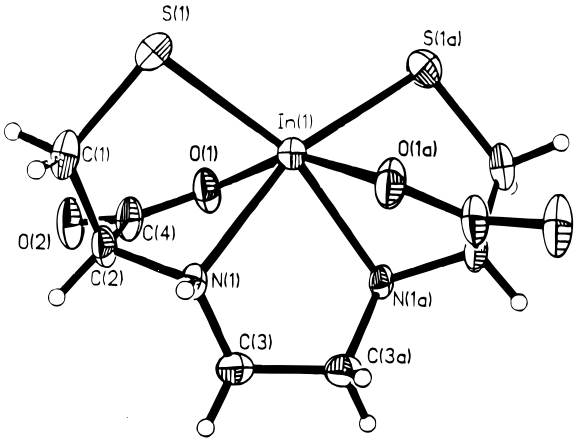

Figure 4. ORTEP diagram of the anion $[InEC]^-$ showing the atom-numbering scheme.

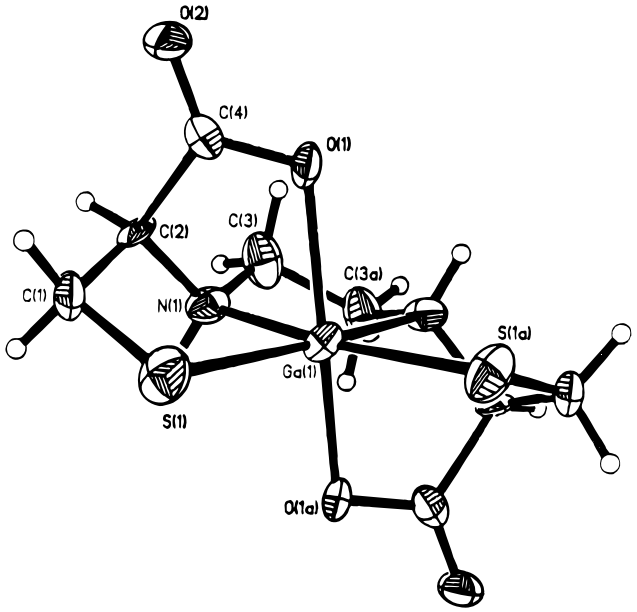

Figure 5. ORTEP diagram of the anion $[GaEC]^-$ showing the atom-numbering scheme.

the first one known for In(III) complexes with cysteine-type ligands.

Figure 5 shows an ORTEP drawing of the complex Na[GaEC]·$2H_2O$, which is similar to that of Na[InEC]·$2H_2O$. The crystal structure of Na[GaEC]·$2H_2O$, like that of the indium complex, is also the first one known for Ga(III) complexes containing cysteine-type ligands. The Ga−O, Ga−N, and Ga−S distances are 2.102(9), 2.115(11), and 2.308(4) Å, respectively. The replacement of the Ga atom with the In atom causes the In−O, In−N, and In−S bond distances to increase by 0.162, 0.166, and 0.144 Å, respectively. These differences, especially for M−S bonds, are smaller than the difference of 0.18 Å[8] between the effective ionic radii of hexacoordinate In^{3+} and Ga^{3+}, reflecting the stronger bonding of In(III)−EC than that of Ga(III)−EC. The replacement of In(III) with Ga(III) causes the unit cell volume to decrease.

The FAB mass spectra of both In(III) and Ga(III) complexes were obtained in a thioglycerol matrix in the negative ion detection mode. The molecular ions from $(MEC - H)^-$, $(MEC + Na - H)^-$ and $(MEC + Na + 2H_2O - H)^-$ (M = In and Ga) were detected. The corresponding molecular weights are 379, 401, and 437 for the In(III) complex and 333, 355, and 391 for the Ga(III) complex, respectively. They are consistent with the solid state structural findings.

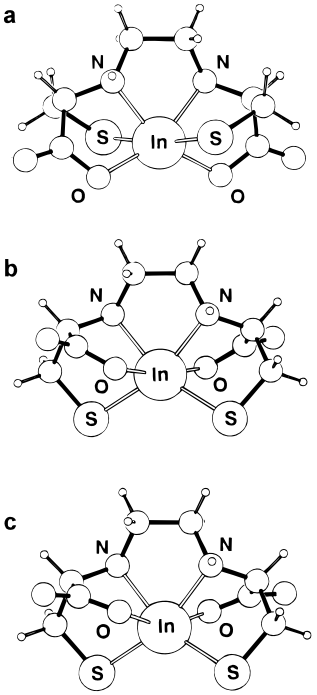

Figure 6. Structures of In(III) complexes of EC as generated by molecular mechanics calculation,[27] and observed. (A) Structure with the sulfur donors *trans* to each other, which has a calculated strain energy of 15.6 kcal.mol^{-1}. (B) Structure with the sulfurs *cis* to each other, which has a calculated strain energy of 8.23 kcal.mol^{-1}. (C) Structure actually observed crystaloographically in this paper. The *cis* and *trans* forms of the Ga(III) complexes with the conformations shown for A and B have strain energies of 8.83 and 13.80 kcal mol^{-1}, respectively.

Molecular Mechanics Calculations. The bond angles and lengths (Table 6b) in the Ga(III) and In(III) complexes with EC and TACN-TM are well reproduced by the force field parameters developed (Table 6a) for In(III) and Ga(III). The structures of other complexes, such as those of EDTA, are also well reproduced by the force field. Using the model building facilities of SYBYL, two conformers of EC complexes with In(III) and Ga(III) were predicted[1] to be of reasonably low energy. These conformers have the two sulfurs of the EC complexes *cis* and *trans* to each other (Figure 6) and are referred to here as the *cis* and *trans* conformers. For both Ga(III) and In(III), the *cis* conformers were predicted[1] to be of lower energy, and the structures observed subsequently (Figures 4 and 5) both have the sulfurs in the *cis* position. For comparison, the structures of the In(III) complex of EC predicted by SYBYL, and observed here, are also shown in Figure 6. The only feature of the In(III) complex not well predicted by the MM calculation is the O−In−O angle. It seems likely that this effect is due to the sulfur donors, since one gains the general impression that donor atoms adjacent to sulfurs are distorted away from the sulfurs, which can be attributed to the large size of the sulfur donor atoms.

The somewhat higher stability of the In(III) complex than of the Ga(III) complex of EC may arise, at least partly, from the slightly higher affinity of In(III) than Ga(III) for sulfur donors, pointed out in the introduction. The strain energies (*PU*) calculated here for the lower energy *cis* complexes of In(III) and Ga(III) with EC are 8.23 and 8.83 kcal mol^{-1} respectively, which may contribute slightly to the greater stability of the In(III) complex. The structures for In(III) and Ga(III) available in the Cambridge Crystallographic Database show that In(III) is usually either octahedral, or seven-coordinate, while Ga(III) is often six-, or sometimes four- or five-coordinate, but never seven-coordinate. The prediction of coordination number is a

matter of some interest in biomedical applications. For example, relaxivity of Gd(III) complexes for magnetic resonance imaging depends[35] on the number of coordinated water molecules, so that whether a proposed Gd(III) complex will add one, two, or no water molecules to its coordination sphere is of interest.

A type of calculation developed[9] for analyzing steric effects as a function of metal ion size can be adapted for predicting coordination numbers. The strain energy (*PU*) of the complex is calculated as a function of M−L bond length, with all other parameters in the force field kept constant. Curves are obtained of strain energy vs M−L length in which the minima correspond to the best-fit size of metal ion, i.e. that size of metal ion which will coordinate with the least steric strain. A modification[36] is to calculate such curves for the same complex with differing numbers of waters coordinated to the metal ion. Families of curves are obtained that have crossover points indicating where, for example, the crowding of the donor atoms around the metal ion is such that six-coordination is sterically less favorable than seven-coordination. Such calculations are based on the work of Kepert,[37] who has shown that coordination geometry of metal ion complexes can be accounted for in terms of simple "points on a sphere" calculations involving repulsion between donor atoms.

EC, EDTA, and TACN-TM are hexadentate ligands. A problem arises for hexadentate ligands that form only five membered chelate rings[5] in coordinating small metal ions, since five membered rings coordinate with less strain to larger metal ions. The metal ion may add extra ligands, such as water molecules, to attain a higher coordination number, and therefore larger ionic radius. This is illustrated by EDTA complexes, where ions such as Mn(II), Fe(III), and In(III) add a unidentate ligand to achieve coordination numbers of seven. In(III) has coordination number seven in several complexes, while no examples of seven coordinate Ga(III) are known. The advantages of the higher coordination number appear to contribute to the higher log K_1 values of EDTA with In(III) (24.9) than Ga(III) (20.3).

MM calculations can be used to analyze the *steric* aspects of coordination number. It has been shown that EDTA, which can form a six-coordinate complex, or with an additional coordinated water molecule to form a seven-coordinate complex, a plot of strain energy vs ionic radius of the metal ion[1] shows that six-coordination is more stable below ionic radius of 0.65 Å, but that a seven-coordinate complex is more stable for metal ions with larger ionic radii, accounting for the fact that the In(III)−EDTA complex is seven-coordinate.[31] For EC, it has been shown[1] that the crossover point from six- to seven-coordinate occurs at 0.82 Å, indicating that the In(III)−EC complex should be six-coordinate, although it is close to the cross-over radius.

The effect of coordination number on complex stability may be important in understanding variations in stability of the types of Ga(III) and In(III) complexes discussed here. A crystal structure[38] of Ga(III) with the tetradentate ligand *N,N′*-bis(2-mercaptoethyl)ethylenediamine is only five coordinate. There is not yet sufficient data to form a clear impression, but it may turn out that ligands of high denticity that only form five membered chelate rings favor In(III), while ligands of lower denticity favor Ga(III). Some data support this idea:

ligand	log K_1(Ga(III))	log K_1(In(III))	denticity of ligand
EDTA	20.3	25.0	6
EC	31.5	33.0	6
MEA[a]	14.81	12.25	2

[a] MEA = (mercaptoethyl)amine, **7**. log K values for MEA from ref 39.

Protonation Constants. There are six donor groups, but only five of them can be protonated within the titratable pH range.

Table 7. Protonation Constants at 25.0 °C and μ = 0.10 M in Aqueous Solution

ligand	log K_1	log K_2^H	log K_3^H	log K_4^H	log K_5^H	ref
EC	11.14(3)	9.88(1)	7.91(2)	5.40(2)	1.7(1)	this work[a]
rac-EHPG	12.05	10.87	8.79	6.44		3
meso-EHPG	11.90	10.85	8.76	6.35		3
HBED	12.63	11.03	8.34	4.40	2.24	4
EDTA	10.13	6.17	2.69	2.12	1.5	7
TACN-TM	13.4	10.97	9.45	8.26	2.50	40
MEA[a]	10.44	8.21				39
cysteine	10.3	8.14				7

[a] MEA = (mercaptoethyl)amine.

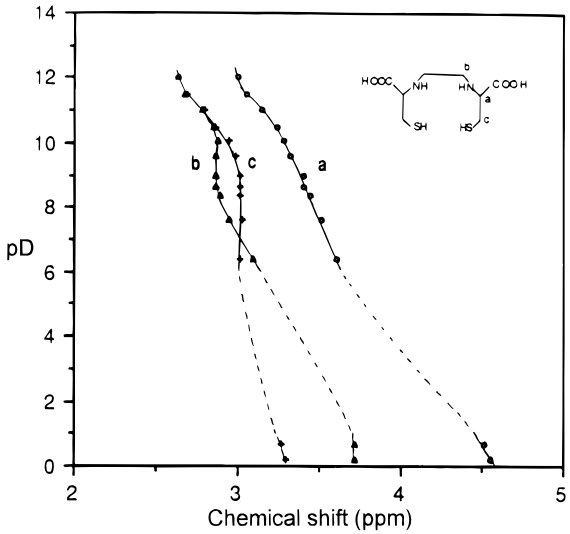

Figure 7. pD dependencies of the ^{1}H NMR chemical shifts in EC−D_2O solution.

The five log protonation constants derived from the potentiometric titration data are 11.14, 9.88, 7.91, 5.40, and 1.7 (Table 7). For the titration curve with ligand alone (Figure 1), the three inflections occurring at a = 0, 1, and 2 separates the curve into three 1-equiv buffer regions (below a = 0, between a = 0 and 1, and between a = 1 and 2) corresponding to the protonation constants $10^{1.7}$, $10^{5.40}$, and $10^{7.96}$, respectively. Also there is a high p[H], 2-equiv buffer region corresponding to the first two high protonation constants. The values of the protonation constants obtained are listed in Table 7, together with the values reported previously for related ligands.

^{1}H NMR titrations of EC were carried out to elucidate the protonation sequence. There are three resonances assigned as *a* (t, −CH−), *b* (s, $-NCH_2CH_2N-$), and *c* (m, $-CH_2S-$) (Figure 7). The assignment of the resonances is straightforward, taking into account the integral area ratio and the pattern of each absorption. Usually each functional group of the ligand may be protonated to a certain degree by addition of 1 equiv of acid. Protonation of the ligand causes the deshielding of the covalently bound hydrogens in the immediate vicinity of the protonated functional group and a shift of the corresponding NMR signals to lower field. The ^{1}H NMR titration curves (Figure 7) show the effect of the successive protonation of the ligand. With the first equivalent of acid added to the deprotonated form of the ligand (between pD 12 and 10.5) all the resonances move downfield by a similar magnitude, suggesting

(35) Lauffer, R. B. *Chem. Rev.* **1987**, *87*, 901.
(36) Hegetschweiler, K.; Hancock, R. D.; Ghisletta, M.; T. Kradolfer, T.; Gramlich, V.; Schmalle, H. W. *Inorg. Chem.* **1993**, *32*, 5273.
(37) Kepert, D. L. *Progr. Inorg. Chem.* **1977**, *23*, 1; **1978**, *24*, 179; **1979**, 25, 41.
(38) Francesconi, L. C.; Liu, B.-L.; Billings, J. J.; Carroll, P. J.; Graczyk, G.; Kung, H. F. *J. Chem. Soc., Chem. Commun.* **1991**, 94.

Scheme 1. Proposed Protonation Sequence of EC

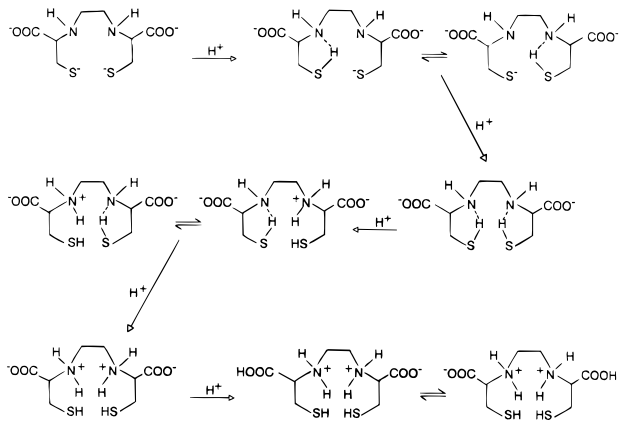

that the protonation takes place on both amino and mercapto groups. The second protonation (pD 10.5−8.5) occurs mainly on the mercapto groups since only resonances a and c move downfield. The third protonation (pD 8.5−6.5) occurs on an amino group, as resonances a and b move downfield. Between pD 6.4 and 1 accurate chemical shifts were not obtained because of low solubility of the ligand in the pD range in which fourth and fifth protonations occur. However, the fourth equivalent of acid certainly protonates the remaining unprotonated amino or mercapto group and the fifth involves the protonation of one of the carboxylate groups. These combined protonation steps cause the largest shift of resonance *a* and the second largest shift of resonance *b*.

The five protonation constants obtained for EC are compared with those of analogous ligands in Table 7. It is seen that the first protonation constant (log $K_1^H = 11.14$) is larger than those of simpler ligands containing mercapto or amino groups such as mercaptoethylamine (MEA, **7**)[7,39] and cysteine (CYS, **8**).[7]

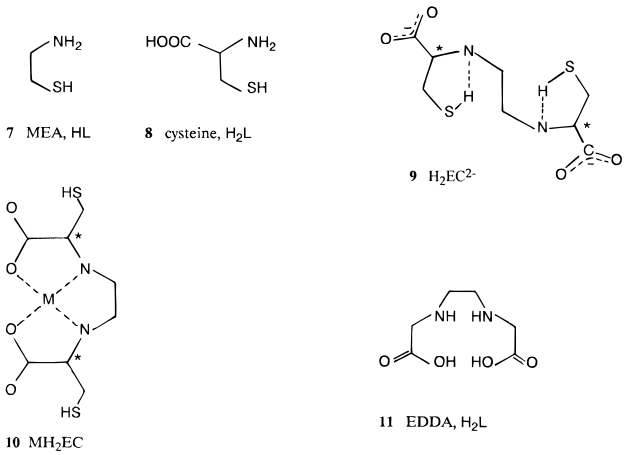

The high protonation constant is probably mainly due to a Coulombic effect. The other ligands which have even higher values of the first and second protonation constants probably have in addition to coulombic effects, hydrogen bonds that stabilize the mono- and diprotonated anions. Hydrogen bonding involving thiolate groups are expected to be much weaker, corresponding to about a log unit lower values of the protonation constants. A possible way in which (weak) hydrogen bonding may be involved in the diprotonated form of the ligand is indicated by formula **9**. It is interesting to note the decrease between the third and fourth protonation constants. The results

(39) Li, Y.; Martell, A. E. *Inorg. Chim. Acta* **1995**, *231*, 159.
(40) Ma, R.; Martell, A. E. *Inorg. Chim. Acta*, in press.
(41) Harris, W. R.; Pecoraro, V. L. *Biochemistry* **1983**, *22*, 292.
(42) Harris, W. R.; Chen, Y.; Wein, K. *Inorg. Chem.* **1994**, *33*, 4991.

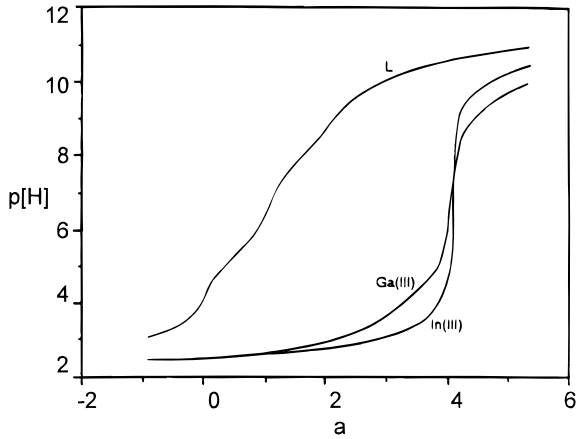

Figure 8. Potentiometric equilibrium curves of 1.00×10^{-3} M EC and EC complexes with trivalent metal ions (as indicated). $t = 25.0$ °C, $\mu = 0.10$ M (KCl), and $a =$ moles of base added per mole of ligand.

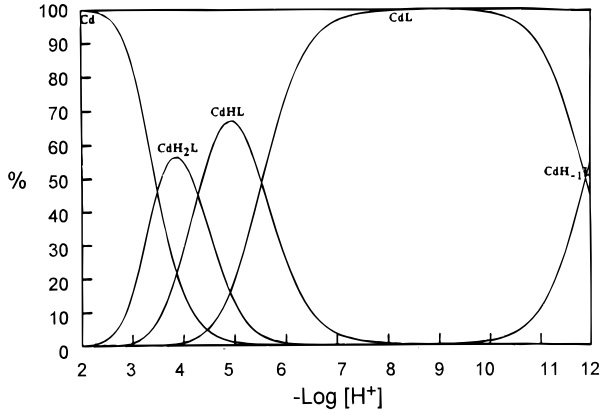

Figure 9. Species distribution curves for 1.00×10^{-3} M Cd(II)−EC system containing a 1:1 molar ratio of Cd(II) to EC. $t = 25.0$ °C; $m = 0.10$ M (KCl); % = percent of species present relative to 1.00×10^{-3} M total EC species = 100%.

of ^{1}H NMR titrations indicate that the fourth constant corresponds to the protonation of the amino group a short distance from another protonated amino group. Thus strong coulombic repulsion exists for the fourth protonation and therefore the fourth protonation constant is a much lower than the third. A protonation sequence (Scheme 1) of EC is suggested on the basis of the results of the ^{1}H NMR and potentiometric titrations. Comparison of the protonation constants of EC with those of the phenolate-containing ligands, EHPG and HBED, shown in Table 7, indicates that the protonation constants of the thiolate groups in EC are lower than those of the phenolate groups in EHPG or HBED, and that the overall basicity of EC is less than that of EHPG or HBED.

Stability Constants. Figures 1 and 8 are the potentiometric equilibrium curves for the formation of divalent and trivalent metal chelates of EC, respectively. All curves have an inflection at $a = 4$, except that of Co(II) which is unique in that no hydroxo species of the Co(II) chelate could be found. This is apparent from visual inspection of the equilibrium curve. Visual inspection of the titration curve also shows that the protonated chelates are the principal species. The 1:1 Co(II) complex CoL^{2-} is not obvious from the equilibrium curves but was required for a computer fit of the data.

It is seen that the computer analysis of the data reveals the existence of mononuclear (1:1) complexes of the divalent metal ions Ni^{2+}, Zn^{2+}, Cd^{2+}, Pb^{2+}, and Co^{2+}. All form monoprotonated chelates, MHL, and diprotonated complex species, MH_2L. Hydroxo complex species were also derived from the titration

Table 8. Logarithms of Stability Constants[a] of Metal Chelates of EC at 25.0 °C and $\mu = 0.10$ M (KCl)

	metal ion						
	Co^{2+}	Pb^{2+}	Cd^{2+}	Zn^{2+}	Ni^{2+}	Ga^{3+}	In^{3+}
$\log K_{ML}$	16.84(4)	19.86(4)	20.87(4)	20.98(4)	24.83(5)	31.5(1)	33.0(1)
$\log \beta_{MHL}$	27.59(2)	27.25(3)	26.41(2)	25.74(2)	28.53(2)	35.89(2)	35.76(3)
$\log \beta_{MH_2L}$	32.58(2).	31.30(4)	30.70(3)	29.92(2)	31.84(4)		
$\log \beta_{MOHL}$		8.40(4)	8.95(3)	9.94(4)	13.44(5)	22.12(2)	22.85(2)
$\log \beta_{M(OH)_2L}$						11.61(4)	11.01(2)
$\log K^{H}_{ML}$	10.75(2)	7.39(3)	5.54(2)	4.76(2)	3.70(2)	4.39(2)	2.76(3)
$\log K^{H}_{MH2L}$	4.99(2)	4.05(4)	4.29(3)	4.18(2)	3.31(4)		
$\log K^{OH}_{MOHL}$		−11.46(4)	−11.92(3)	−11.04(4)	−11.39(5)	−9.38(2)	−10.15(2)
$\log K^{OH}_{M(OH)2L}$						−10.51(4)	−11.84(2)
$\log K_{MH_2L}$[a]	11.55(4)	10.27(3)	9.68(3)	8.59(3)	10.81(5)		

[a] $K_{MH_2L} = [MH_2L]/[M^{2+}][H_2L^{2-}]$.

Table 9. Logarithms of Stability Constants of Divalent Metal Complexes of EC and Related Ligands

ligand	equilibrium quotient	Co(II)	Pb(II)	Cd(II)	Zn(II)	Ni(II)
EC	$[ML^{2-}]/[M^{2+}][L^{4-}]$	16.84(4)	19.86(4)	20.87(4)	20.98(4)	24.83(5)
	$[MH_2L]/[M^{2+}][H_2L^{2-}]$	11.55	10.27	9.68(3)	8.59(3)	10.81(5)
rac-EHPG[a]	$[MH_2L]/[M^{2+}][H_2L^{2-}]$				9.06	11.33
meso-EHPG[a]	$[MH_2L]/[M^{2+}][H_2L^{2-}]$				9.24	11.19
EDDA[b]	$[ML]/[M][L]$	11.23	10.7	9.1	11.1	13.65
cysteine[b]	$[ML_2^{2-}]/[M^{2+}][L^{2-}]^2$	14.2	15.9	16.89	18.12	20.07

[a] Reference 3. [b] Reference 7.

data, except for Co(II). In(III) and Ga(III) complexes form dihydroxo species as well as monohydroxo chelates.

After various combinations of likely species were investigated, the formation constants in (1)−(5) were found to

$$M^{2+} + L^{4-} \rightleftharpoons ML^{2-}\ K_{ML} = [ML^{2-}]/[M^{2+}][L^{4-}] \quad (1)$$

$$M^{2+} + H^{+} + L^{4-} \rightleftharpoons MHL^{-}\ \beta_{MHL} = [MHL^{-}]/[M^{2+}][H^{+}][L^{4-}] \quad (2)$$

$$M^{2+} + 2H^{+} + L^{4-} \rightleftharpoons MH_2L\ \beta_{MH_2L} = [MH_2L]/[M^{2+}][H^{+}]^2[L^{4-}] \quad (3)$$

$$M^{2+} + OH^{-} + L^{4-} \rightleftharpoons MOHL^{3-}\ \beta_{MOHL} = [MOHL^{3-}]/[M^{2+}][OH^{-}][L^{4-}] \quad (4)$$

$$M^{2+} + 2OH^{-} + L^{4-} \rightleftharpoons M(OH)_2L^{4-}\ \beta_{M(OH)_2L} = [M(OH)_2L^{4-}]/[M^{2+}][OH^{-}]^2[L^{4-}] \quad (5)$$

completely reproduce the potentiometric equilibria. The reactions 2−5 may be rewritten as reactions 6−9.

$$ML^{2-} + H^{+} \rightleftharpoons MHL^{-}\ K^{H}_{MHL} = [MHL^{-}]/[ML^{2-}][H^{+}] \quad (6)$$

$$MHL^{-} + H^{+} \rightleftharpoons MH_2L\ K^{H}_{MH_2L} = [MH_2L]/[MHL^{-}][H^{+}] \quad (7)$$

$$ML^{2-} + H_2O \rightleftharpoons M(OH)L^{3-} + H^{+}\ K^{OH}_{MOHL} = [MOHL^{3-}][H^{+}]/[ML^{2-}] \quad (8)$$

$$M(OH)L^{3-} + H_2O \rightleftharpoons M(OH)_2L^{4-} + H^{+}\ K^{OH}_{M(OH)_2L} = [M(OH)_2L^{4-}][H^{+}]/[M(OH)L^{3-}] \quad (9)$$

The equilibrium constants defined by eqs 1−9 are given in Table 8. The constants for In(III) and Ga(III) complexes of EC are also listed in the same table. The relative order of stabilities of the metal complexes with EC are In(III) > Ga(III) ≫ Ni(II) > Zn(II) > Cd(II) > Pb(II) > Co(II).

The protonated forms of the divalent metal complexes predominate in acid solution as indicated by the data in Table 8 and by the species distribution curves (for example : Cd(II) complexes in Figure 9) . The first two protonation sites are assigned to the mercapto groups. A probable arrangement of ligand donor groups of the diprotonated form is shown in formula **10**, in which the two asymmetric carbon atoms with the L configuration are indicated by an asterisk and the metal ion is coordinated by two amino and two carboxylate groups. Comparison with the analogous chelates of EDDA, *N,N′*-ethylenediaminediacetic acid, **11**, indicates that the arrangement of donor groups in formula **10** may apply to the Co(II), Pb(II), and Cd(II) diprotonated complexes of EC because their stabilities are close to those of EDDA. But significantly lower stability constants are observed for the diprotonated Ni(II) and Zn(II) complexes of EC (Table 9) compared to the stabilities of the EDDA complexes. The stability constants of corresponding diprotonated complexes of EHPG are also significant lower than those of EDDA complexes. A different arrangement of donor groups of the diprotonated form must be involved in the Ni(II) and Zn(II) complexes. Participation of the mercapto donor groups of EC in metal ion coordination greatly increases the stability constant especially in the case of Ni^{2+} and Zn^{2+}, which have high affinity for S^{-} donors. The stability constant of $10^{24.83}$ for Ni(II)-EC complex is the highest one among the divalent metal complexes studied in this work and of the other ligands listed in Table 9.

The stability sequence of monoprotonated divalent metal complexes (Table 8) is in agreement with the concept that the higher the stability of the complex, the lower is the protonation constant. This is logical since the greater the interaction between a ligand donor group and a metal ion, the lower is its tendency to combine with a competing positive ion.

It is noted that the stability constants of the hexadentate complexes of EC are greater than the overall stability constants of bis-tridentate complex of cysteine for all divalent metal ions listed in Table 9. The stability constants of related ligands are compared in Table 9.

Both In(III) and Ga(III) react strongly with the ligand and at considerably lower pH than do the divalent metal ions. Inspection of the lower buffer regions of the p[H] profiles (Figure 8) indicate the presence of significant concentrations of proto-

Table 10. Formation Constants and pM Values at Physiological pH for Ga(III) and In(III) Complexes[a]

Ga(III) ligand	In(III) log K_{ML}	pM	log K_{ML}	pM
EC	31.5	24.7	33.0	26.2
TACN-TM	34.2	23.6	36.1	23.9
HBED	38.51	28.6	27.76	17.9
EDTA	21.0	20.7	24.9	22.2
transferrin[b]	20.3[c], 39.6[c,d]	20.4	18.3[c], 35.1[c,d]	18.3

[a] $t = 25.0$ °C; $\mu = 0.10$ M (KCl); pM = −log [M] at pH 7.4 and 100% excess ligand. [b] References 41 and 42. [c] Conditional constants at p[H] 7.4. [d] log β_{M_2L}.

nated chelates as well as nearly complete coordination of indium and gallium. The stability constants of the 1:1 ML chelates were derived from the p[H] titration of the competition reaction with EDTA for In(III)−EC and Ga(III)−EC, respectively (not shown). For the Ga(III) system, EDTA competes with EC below pH 6 but only predominates below p[H] 3. For In(III) the competition occurs in the p[H] range 3−7.5. The In(III)−EDTA complex predominates at and below p[H] 5.0.

The stabilities of a number of Ga(III) and In(III) chelates are compared in Table 10. Correlations of In^{3+} *in vivo* behavior, measured by its binding to transferrin with stability constants (log *K*) are not possible because stability constants express the metal ion affinity for a completely deprotonated ligand, whereas the transferrin constants are conditional ones at physiological pH (taken here as 7.4). On the other hand the effectiveness of ligands in binding metal ions may be more suitably compared by considering pM (−log [M]) as a direct measure of the concentration of free metal ion present at the p[H] of interest.

The pM values of Ga(III)−EC and In(III)−EC are 4 and 8 log units larger than those of Ga(III)−transferrin and In(III)−transferrin, respectively (Table 10). Therefore the competition between EC and transferrin for either Ga^{3+} or In^{3+} is seen to be completely in favor of EC at p[H] 7.4, indicating that the complexes should be stable enough to avoid interference by transferrin. The radiolabled complexes of ^{111}InEC and ^{67}GaEC were recently confirmed to be stable *in vivo*.[1] The pM values for the Ga(III)−HBED complex is much higher than for the In(III) complex, while the pM value for In(III) is close to that of In(III)−transferrin. This would indicate some extent of metal ion exchange with transferrin for the In(III)−HBED−transferrin system. Even though the stability constants[1] for TACN-TM (1,4,7-tris(2-mercaptoethyl)-1,4,7-triazacyclononane) (N_3S_3) chelates are larger than those of the corresponding EC chelates, the pM values for Ga(III) and In(III)−TACN-TM complexes at physiological pH (7.4) are 1−2 log units less than those of In(III)−EC and Ga(III)−EC, respectively, because TACN-TM has high protonation constants, and therefore formation of its complexes are subject to stronger hydrogen ion competition. EC containing thiolate donors is a more effective multidentate ligand and potential radiopharmaceutical in the form of the ^{111}In complex than the corresponding complexes of HBED or TACN-TM.

High stability is an important prerequisite for potential $^{67}Ga^{3+}$ or $^{111}In^{3+}$ complexes used as radiopharmaceuticals. The fact that In(III) and Ga(III) complexes of EC are very stable in aqueous solution, do not dissociate at physiological p[H] (7.4), and do not exchange with transferrin to an appreciable extent, indicates that it may be an effective ligand for radiopharmaceutical applications. The high stabilities may reflect the strong bonding associated with the metal thiolate coordinate bonds, especially for the In(III) complex. However, the ligand EC produces anionic complexes when it chelates to In(III) or Ga(III). Such charged complexes are generally low in lipophilicity and may have poor membrane permeability. The present results may lead to further development of mercaptide-containing ligands that would be able to form highly lipophilic and stable complexes with In(III) and Ga(III).

Acknowledgment. This work was supported by grants from the National Cancer Institute, U.S. Public Health Service, No. CA-42925, and The Robert A. Welch Foundation, No. A-259.

Supporting Information Available: Complete crystal data and structure refinement (Table S1), atomic coordinates and equivalent isotropic displacement parameters (Table S2), bond lengths and angles (Table S3), anisotropic displacement parameters (Table S4), hydrogen coordinates and isotropic displacement parameters (Table S5), and packing diagrams of **I**, **II**, and **III** (19 pages). Ordering information is given on any current masthead page.

IC941330L